Heterogeneous Phosphotungstate Catalyst Mediated Efficient Alcoholysis of Furfuryl Alcohol into Long-Chain Levulinates

Yinghui Wang, Jiao Ma, Qiang Zheng, Yali Ma, Songyan Jia,* and Xue Li *

The synthesis of alternative fuels from biomass has emerged to be a vital strategy to maintain sustainable development. Long-chain levulinate esters (LEs) are a class of good biofuel candidates because they have similar structures to biodiesels and superior heating values. The synthesis of long-chain LEs with effective heterogeneous catalysts has always been challenging. In this work, a few heterogeneous phosphotungstate catalysts were facilely prepared, among which the V^{3+} exchanged phosphotungstic acid catalyst (VPW) was the most active for the alcoholysis of furfuryl alcohol (FA) and 1-hexanol into 1-hexyl levulinate (HL). A maximum HL yield of 63% was achieved at 180 °C. The VPW catalyst could be reused without obvious decrement of activity. The system was also applicable to the alcoholysis of FA with other hexanols and 1-octanol into various long-chain LEs.

DOI: 10.15376/biores.18.3.5765-5776

Keywords: Long-chain levulinate; Heterogeneous phosphotungstate; Furfuryl alcohol; Liquid fuel

*Contact information: College of Chemical Engineering, Liaoning Engineering Research Center for Magnesium and Calcium Inorganic Functional Materials, Shenyang Key Laboratory for the Utilization Technology of Magnesium and Calcium Resources, Shenyang University of Chemical Technology, Shenyang Liaoning, 110142, China; *Corresponding authors: jiasongyan@126.com; ltmlx@163.com*

INTRODUCTION

Energy shortage and climate change are currently core concerns for the whole world (Clarke and Wei 2020). The carbon-neutral concept has already been proposed and practiced in many countries, primarily depending on the widespread application of clean renewable energies (Liao *et al*. 2022). Biomass is considered as a potential energy source that can provide renewable carbon. Thus, the efficient valorization of biomass is a reliable strategy to relieve reliance on the traditional energies (Li *et al*. 2016).

Fossil fuels are the major emission source of greenhouse gas (Zhang and Li 2022). Biomass possesses the carbon-neutral property by photosynthesis (Saravanakumar *et al*. 2023). As such, acquiring fuels from biomass can significantly achieve the reduction of carbon footprints. Levulinate esters (LEs) are a class of promising biomass-based fuel chemicals (Di *et al*. 2022). The LEs contain an appropriate amount of oxygen, which is conducive to promote combustion and reduce the emissions of NOx and particulate pollutants (Christensen *et al*. 2011). Nevertheless, many works currently focus more on the synthesis of short-chain levulinates such as methyl and ethyl levulinates (Liang *et al*. 2020; Kim and Han 2021; Du *et al*. 2022). In previous works, the authors elucidated that long-chain levulinates (C_{11+}) have similar structures to biodiesels and their lower heating values are close to gasoline (Jia *et al*. 2020b, 2022). In addition, long-chain LEs have lower toxicity than short-chain ones (Lomba *et al*. 2014). However, information on the efficient synthesis of long-chain LEs remains lacking.

The LEs can be produced through three approaches, including the esterification of levulinic acid, the alcoholysis of furfuryl alcohol (FA), and the conversion of saccharides (Yang *et al*. 2019; Jia *et al*. 2020a; Chung *et al*. 2022). The alcoholysis of FA affords more efficiency, while the other two approaches suffer from either longer processing periods to gain levulinic acid or more side reactions from the direct conversion. The FA is a hydrogenation product from furfural, a popular platform compound from hemicellulose. Acidic materials represent the common catalysts for the alcoholysis of FA, such as inorganic acids, metal salts, ionic liquids, and various functionalized materials (Peng *et al*. 2014; Wang *et al*. 2014; Peng *et al*. 2015; Zhou *et al*. 2022). Inorganic and organic acids are homogeneous catalysts, which suffer separation and waste disposal issues. Both metal salts and ionic liquids also primarily serve as homogeneous catalysts, having some similar problems as above. The heterogeneous catalysts are more desirable due to a few merits such as the reduction of cost and waste disposal by recycling. The heterogeneous catalysts usually face the challenges of complex preparation process and the stabilization of activity. The regeneration of a deactivated catalyst is also a crucial topic. The designing of facilely prepared and active heterogeneous catalysts is an urgent project in the area of FA alcoholysis. Heteropolyacids are a type of strong acid catalyst and have been applied in biomass conversion, including the alcoholysis of FA (Sankar *et al*. 2017; Tiwari *et al*. 2020). However, the regular heteropolyacids are well soluble in water and some organic solvents, so they work more frequently as homogeneous catalysts. According to previous works, the introduction of cations with a large ionic radius can heterogenize the heteropolyacids while preserving appropriate acidities, of which the synthesis procedure is facile (Zhang *et al*. 2011; Zhou *et al*. 2016). Therefore, this kind of heterogeneous heteropolyacid salt catalyst may have good potential in the synthesis of long-chain LEs by FA. It is worth mentioning that the complexation strength between cations and heteropolyate anions is a key factor, which may affect the catalyst activity.

This study was devoted to the efficient synthesis of long-chain LEs with facilely prepared heterogeneous catalysts. A number of heterogeneous phosphotungstates were synthesized, characterized, and tested for the alcoholysis of FA. 1-Hexanol was employed as the primary alcoholysis reagent. Reaction parameters, such as catalyst loading, molar ratio of feedstocks, reaction temperature, and time, were studied in detail. The catalyst reusability and the adaptability for other long-chain alcohols were also evaluated.

EXPERIMENTAL

Materials

Furfuryl alcohol (98%), phosphotungstic acid ($H_3PW_{12}O_{40}$, 98%), vanadium(III) chloride (VCl_3, 97%), chromium(III) chloride hexahydrate ($CrCl_3•6H_2O$, 98%), γ-valerolactone (GVL, 99%), *p*-xylene (99%) and *p*-nitroaniline (99%) were all purchased from Aladdin (Shanghai, China). The 1-hexanol (99%), 2-hexanol (99%), 3-hexanol (99%), 2-ethyl-1-butanol (99%), cyclohexanol (99%), 1-octanol (99%), iron(III) chloride ($FeCl_3$, 99%), and copper (II) chloride dehydrate ($CuCl_2•2H_2O$, 99%) were all purchased from Energy Chemical (Shanghai, China). All the reagents were used as received.

Catalysts Preparation

$H_3PW_{12}O_{40}$ was used as the motif, of which the proton was exchanged by metal cations including V^{3+}, Fe^{3+}, Cr^{3+}, and Cu^{2+}. For instance, 4 mmol of $H_3PW_{12}O_{40}$ and VCl_3 were added into a flask with 20 mL of water. The solution was stirred thoroughly at 40 °C for 6 h, after which the mixture was aged in a Teflon reactor at 140 °C for 24 h. Next, the mixture was dried at 60 °C, and dark green solid was gained. The solid was calcined at 350 °C for 3 h with a heating rate of 5 °C/min from 50 °C. The final product was labeled as VPW. Similarly, $FeCl_3$, $CrCl_3 \bullet 6H_2O$, and $CuCl_2 \bullet 2H_2O$ were used to prepare the catalysts. It should be noted that 6 mmol of $CuCl_2 \bullet 2H_2O$ was used to exchange the protons due to the balancing of valence. The above three as-synthesized catalysts were labeled as FePW, CrPW, and $Cu_{1.5}PW$, respectively.

Typical Reaction Procedure

Typically, 1 mmol of FA, 9 mmol of 1-hexanol and 1 mL of GVL solvent were added into a reaction vial with a catalyst (30 wt% to FA). GVL was used as the solvent to reduce the possible self-polymerization of FA to some extent. The sealed vial was inserted into a heating and stirring module for reaction at a certain temperature. Once reaching the reaction time, the vial was taken out and placed into a cold water bath to quench the reaction. A total of 2 mL of acetone was added to dilute the reaction mixture, and 0.1 mmol of *p*-xylene was added as the internal standard for calculation. The final mixture was centrifuged, then the supernatant liquid was filtered using a syringe-driven filter and analyzed by a gas chromatography (GC) instrument. All the conversion experiments were repeated three times, and the average data were used for discussions.

Analysis Method

X-ray diffraction (XRD) was performed on a Panalytical Empyrean system (PANalytical B.V., Almelo, Holland). Fourier transform infrared spectroscopy (FT-IR) was performed on a Thermo Scientific Nicolet iS20 system (Thermo Nicolet Corporation, Madison, WI, USA). Ammonia temperature-programmed desorption (NH_3-TPD) was performed on a Quantachrome ChemBET Pulsar chemisorption apparatus (Anton Paar, Graz, Austria). Ultraviolet-visible (UV-vis) spectra were recorded on a Shimazu UV 2550 spectrophotometer (Shimazu Corporation, Kyoto, Japan).

The gas chromatography (GC) tests were performed on a Hanwei brand (Hanwei Electronics Group Corporation, Zhengzhou, China) GC-L96 system with a flame ionization detector and a SE-54 capillary column (30 m × 0.32 mm × 0.5 μm). The carrier gas was nitrogen. The temperatures of the vaporization chamber and detector were both set at 250 °C. The column was maintained at 120 °C for 1 min. It then was heated to 200 °C with a heating rate of 30 $°C \bullet min^{-1}$ and maintained at 200 °C for 4 min. The FA conversion and levulinate ester yield were calculated according to Eqs. 1 and 2 below:

$$\text{FA conversion (mol\%)} = (1 - \text{FA residue/initially added FA}) \times 100\% \quad (1)$$

$$\text{LE yield (mol\%)} = (\text{detected ester/ideal amount of ester by initial FA}) \times 100\% \quad (2)$$

The detailed formulas for the calculations were given in the supplementary file.

RESULTS AND DISCUSSION

Catalyst Characterization

Some metal cations, such as V^{3+}, Fe^{3+}, Cr^{3+}, and Cu^{2+}, were chosen to synthesize the catalysts because they had shown good activities by Lewis acidity in biomass conversion (Sádaba *et al*. 2011; Zhang *et al*. 2014; Xu *et al*. 2018; Zhang *et al*. 2021). Figure 1 shows the XRD patterns of $H_3PW_{12}O_{40}$ and the as-synthesized catalysts. The peaks at 2θ of around 10°, 18°, 21°, 23°, 26°, 30°, 35°, 38°, 53°, and 60° represent the characteristics for the Keggin structure of $H_3PW_{12}O_{40}$ (Pasha *et al*. 2019). Some subtle differences were observed, possibly because of the exchange of metal cations.

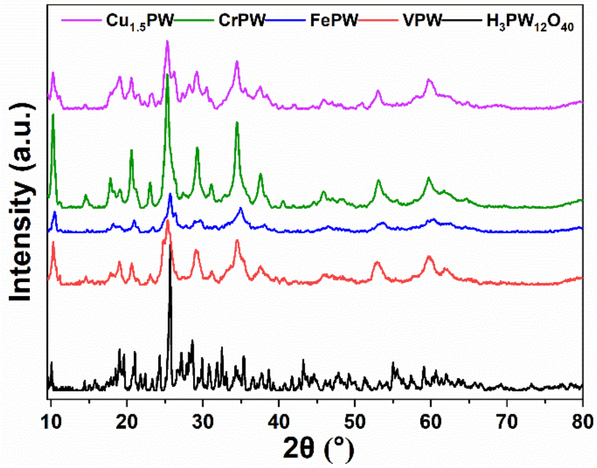

Fig. 1. XRD patterns of $H_3PW_{12}O_{40}$ and the as-synthesized catalysts

The FT-IR spectra of $H_3PW_{12}O_{40}$ and the as-synthesized catalysts are illustrated in Fig. 2. The band at about 1080 cm^{-1} could be attributed to the stretching vibration of tetrahedral P-O bond. The band at about 990 cm^{-1} accounted for the stretching vibration of W=Ot bond, of which the Ot represents the terminal oxygen. The bands at about 890 and 800 cm^{-1} were ascribed to W-Oc-W and W-Oe-W, where Oc and Oe represent the corner sharing oxygen and the edge sharing oxygen, respectively (Pasha *et al*. 2019).

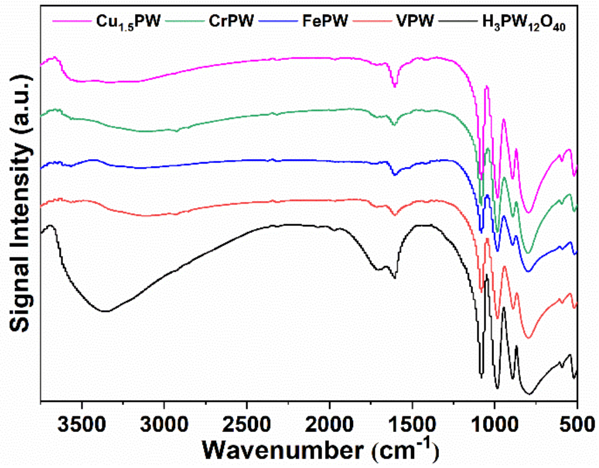

Fig. 2. FT-IR spectra of $H_3PW_{12}O_{40}$ and the as-synthesized catalysts

The catalysts exhibited similar characteristic bands to $H_3PW_{12}O_{40}$ at the range of 750 to 1250 cm^{-1}, indicating that the Keggin structures were maintained. $H_3PW_{12}O_{40}$ showed a remarkable absorbance at about 3400 cm^{-1}, which was attributed to the –OH group. The disappearance of the band at about 3400 cm^{-1} for the catalysts demonstrated that the protons in –OH groups of $H_3PW_{12}O_{40}$ had been well substituted by the above metal cations. Figure S1 illustrated the Energy Dispersive Spectroscope (EDS) analyses of the catalysts, which also confirmed the existence of these metal species.

Figure 3 illustrates the acidic strengths of $H_3PW_{12}O_{40}$ and the as-synthesized catalysts by NH_3-TPD and UV-vis analyses. Figure 3a shows that all the catalysts gave NH_3 desorption signals at about 120 to 170 °C, which indicated that the catalysts possessed weak acidic species with a strength order as $Cu_{1.5}PW \approx H_3PW_{12}O_{40} > CrPW > FePW > VPW$. For comparison, the acidities of $H_3PW_{12}O_{40}$ and the four catalysts were also tested by UV-vis spectrophotometry according to a literature (Yang and Kou 2004). In short, a *p*-nitroaniline aqueous solution with a concentration of 2.9 mmol·L^{-1} was made. Then, 0.1 mmol of $H_3PW_{12}O_{40}$ or catalyst was each added into the above solution. The weak UV absorption of *p*-nitroaniline represents the strong acidity. As seen in Fig. 3b, the UV-vis spectra gave a similar acid strength order to NH_3-TPD results.

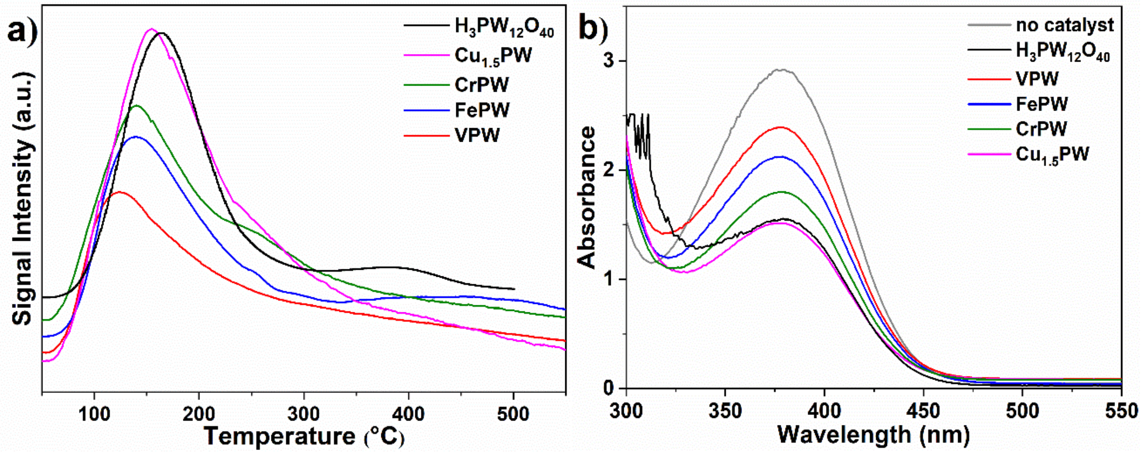

Fig. 3. NH_3-TPD analyses (a) on $H_3PW_{12}O_{40}$ and the catalysts and UV-vis analyses (b) on the aqueous solutions of *p*-nitroaniline with $H_3PW_{12}O_{40}$ and the catalysts

Catalytic Alcoholysis of FA into Long-chain Levulinates

The catalysts were screened for the alcoholysis of FA with 1-hexanol as an esterification reagent. The tests were conducted at 140 °C for 180 min with a catalyst amount of 30 wt% (to FA). The initial molar ratio of 1-hexanol/FA was 9, and 1 mL of GVL was used as the solvent. As seen in Fig. 4, the alcoholysis of FA and 1-hexanol could proceed even in the absence of a catalyst with a 1-hexyl levulinate (HL) yield and selectivity of 24% and 29%, respectively. Some water could be produced by the condensation of FA (Alimukhamedov and Magrupov 2007), and FA may react with water to form a small amount of organic acid such as levulinic acid at high temperature (Hronec *et al.* 2014). As such, the possibly produced organic acid was speculated to work as a catalyst to a certain degree. The FA conversion reached 84%, indicating that more side-reactions occurred. As reported, FA could undergo self-polymerization, which is one reason for the high conversion (Kim *et al*. 2013). When $H_3PW_{12}O_{40}$ was used as the catalyst, a FA conversion of 85% and a HL yield of 40% were obtained. The as-synthesized catalysts had different activities, among which VPW showed a better efficiency with a HL yield and selectivity of 49% and 57%, respectively. Although the as-synthesized catalysts showed a close activity to $H_3PW_{12}O_{40}$, they exhibited heterogeneous character, having the potential for reuse. According to the results of NH_3-TPD and UV-vis analyses, VPW catalyst was the relatively least acidic, indicating that stronger acidity may lead to more side reactions. Moreover, the as-synthesized catalyst appeared to be heterogeneous in the system, implying the superior reusability to $H_3PW_{12}O_{40}$. Therefore, VPW was selected as the optimal catalyst for further investigations.

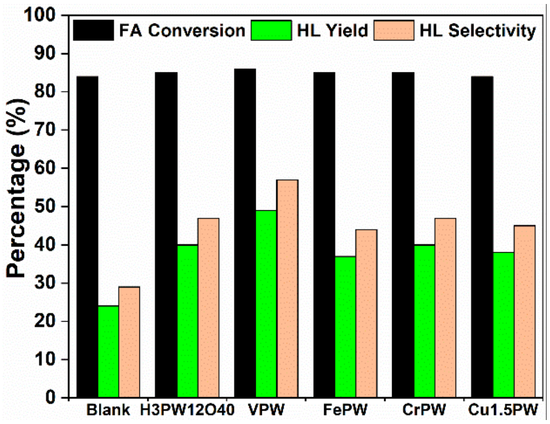

Fig. 4. Comparison on the alcoholysis of FA with 1-hexanol over different catalysts

Figure 5 illustrates the effects of VPW usage and FA/1-hexanol molar ratio on the alcoholysis of FA into HL at 140 °C for 180 min. As shown in Fig. 5a, when 10 wt% of VPW was added, the actual improvement on the production of HL was insignificant compared to the blank test. With the increment of catalyst, HL yield and selectivity clearly increased, while excess catalyst may also accelerate some side-reactions, resulting in the decrement of HL yield and selectivity. As such, the catalyst loading of 30 wt% was used as an optimal dosage.

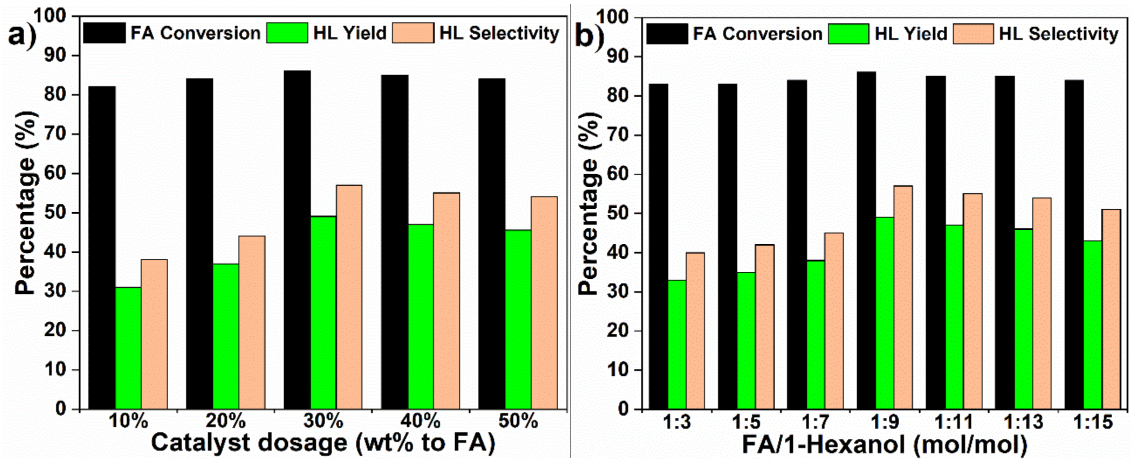

Fig. 5. Effects of catalyst loading (a) and feedstock molar ratio (b) on the alcoholysis of FA

The alcoholysis of FA into levulinates is a stoichiometric reaction. One of the feedstocks is excessively used to drive the reaction forward. To circumvent the self-polymerization of FA, 1-hexanol was excessively added. As shown in Fig. 5b, increasing the usage of 1-hexanol did not affect the conversion of FA much, while the production of HL was remarkably improved. When the FA/1-hexanol ratio was 1:9, the HL yield and selectivity reached 49% and 57%, respectively. However, further increasing the loading of 1-hexanol may lead to a slight drop of HL yield and selectivity. The catalyst concentration in the mixture could be diluted by the continual addition of 1-hexanol, thereby leading to the decrement of reaction performance.

To obtain an optimal reaction performance, the alcoholysis of FA and 1-hexanol was monitored as a function of reaction time at different temperatures. As illustrated in Fig. 6, FA conversion showed a different trend from HL yield. The FA underwent fast conversion at the level of approximately 85 to 90% within a short time, which was not affected by temperature. Elevating the reaction temperature considerably promoted the production of HL. A maximum HL yield of 63% was acquired at 180 °C after 180 min, while prolonging time could also lead to more side reactions and reduce HL yield in a way. As seen in Fig. 6, the conversion of FA was much faster than the production of HL, indicating that FA could first transform into a certain intermediate, which underwent the subsequent conversion to produce HL gradually. The authors conducted two control experiments to understand how the intermediates formed. First, the VPW catalyst was mixed with 1-hexanol or FA in GVL at 140 °C for 60 min. Then, another reactant was added to react for 60 min. When 1-hexanol was mixed with VPW prior to the addition of FA, no unusual conversion occurred. The FA conversion and HL yield were 84% and 37%, respectively, very close to those regular data (as seen in Fig. 6b). As compared, when FA was first mixed with VPW, only a HL yield of 24% was obtained, indicating that the intermediates could be formed by the interaction of FA and catalyst.

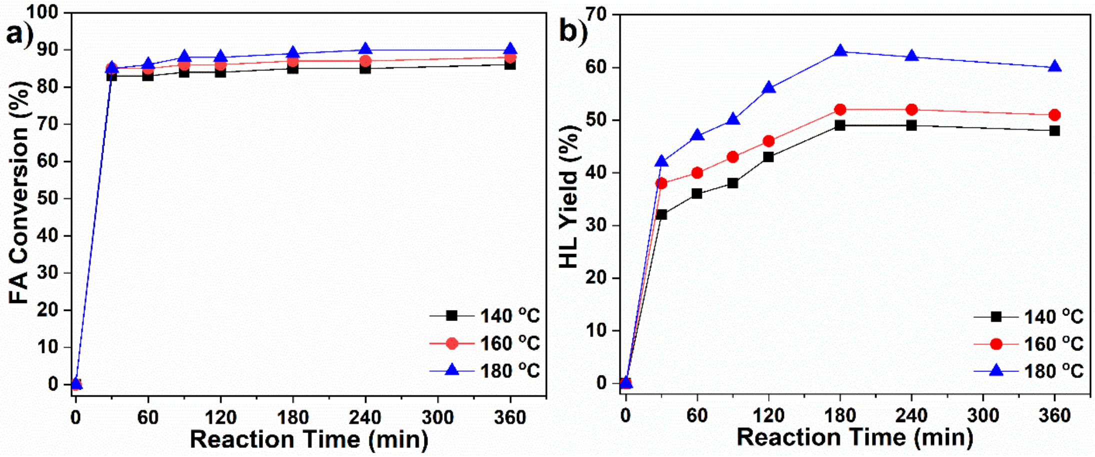

Fig. 6. The alcoholysis of FA and 1-hexanol into HL at different temperatures

Stability and reusability are highly desirable for a heterogeneous catalyst. The authors also studied the recycling of VPW catalyst for the alcoholysis of FA. The tests were conducted under the optimal conditions. After each run, the catalyst was filtered out and dried before the next run. As shown in Fig. 7, apparently the VPW showed good reusability with only slight decrease of HL yield and selectivity.

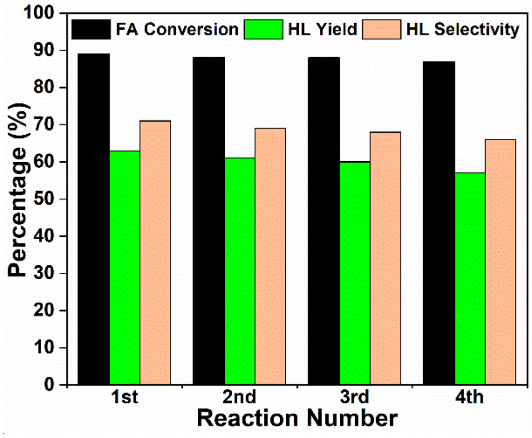

Fig. 7. The recycling test on the alcoholysis of FA and 1-hexanol over VPW catalyst

The Alcoholysis of FA with Various Hexanols and 1-Octanol

As discussed, long-chain LEs are potential biobased fuel chemicals (Lomba *et al*. 2014; Jia *et al*. 2020a, 2022b). However, HL is only a representative long-chain LE. The synthesis of various long-chain LEs is conducive to tune the octane number of these fuel chemicals. To explore this point, the alcoholysis of FA with some other hexanols and 1-octanol as a longer chain alcohol were reinvestigated. As listed in Table 1, when 2-hexanol or 3-hexanol was used, the corresponding levulinate yield was lower than that with 1-hexanol (Fig. 6b). The alcoholysis of FA is affected by the steric hindrance of the hydroxyl group of an alcohol (Gupta and Kantam 2019). Both 2-hexanol and 3-hexanol are secondary alcohols, which possibly accounts for the inferior product yields. 2-Ethyl-1-butanol itself is a primary alcohol, so the alcoholysis of FA and 2-ethyl-1-butanol is similar to that with 1-hexanol. Although cyclohexanol is a secondary alcohol, the fixed six-membered ring structure makes the hydroxyl group more naked, resulting in a smaller steric hindrance and a relatively high yield of levulinate. Elevating the reaction temperature could improve the alcoholysis of FA with 2-hexanol and 3-hexanol. Moreover, 1-octanol was employed as a longer chain alcohol for the alcoholysis of FA. A comparable yield of 1-octyl levulinate was obtained. The larger steric hindrance by the octyl group may lead to a slightly lower product yield.

Table 1. Results on the Alcoholysis of FA with Hexanols and 1-Octanol

Entry	Alcohol	Temperature (°C)	FA Conversion (%)	Levulinate Yield (%)
1	2-hexanol	140	85	36
2	2-hexanol	160	86	46
3	3-hexanol	140	85	34
4	3-hexanol	160	87	45
5	2-ethyl-1-butanol	140	84	51
6	cyclohexanol	140	84	50
7	1-octanol	140	85	45
Note: Conditions: 1 mmol FA, 9 mmol alcohol, VPW catalyst 30 wt% to FA, 1 mL GVL, 180 min				

CONCLUSIONS

1. In this work, the authors facilely prepared a few heterogeneous phosphotungstate catalysts, among which the one exchanged by V^{3+} (VPW) was the most active for the alcoholysis of furfuryl alcohol (FA) and 1-hexanol into 1-hexyl levulinate (HL). A maximum HL yield of 63% could be obtained at 180 °C after 180 min.
2. The VPW catalyst showed good stability and reusability. The system was also suitable for the alcoholysis of FA with various hexanols and longer chain alcohol.
3. The alcoholysis reaction may proceed *via* some certain intermediate produced by the interaction between FA and VPW catalyst.

ACKNOWLEDGMENTS

This work was supported by the Natural Science Foundation of Liaoning Province (China) (2019-ZD-0083 and 2022-BS-210), Department of Education of Liaoning Province (China) (LQ2020001 and LQ2020003), Joint Fund for Innovation Enhancement (2021-NLTS-12-04), and Intercollegiate Cooperation Program for Undergraduate University of Liaoning Province (China) (2020-28).

REFERENCES CITED

Alimukhamedov, M. G., and Magrupov, F. A. (2007) "Kinetics of homopolycondensation of furfuryl alcohol," *Polymer Science B* 49, 167-171. DOI: 10.1134/S1560090407070019

Chung, S. H., De Haart, S., Parton, R., and Shiju, N. R. (2022). "Conversion of furfuryl alcohol into alkyl-levu/linates using solid acid catalysts," *Sustainable Chemistry for Climate Action* 1, article ID 100004. DOI: 10.1016/j.scca.2022.100004

Clarke, L., and Wei, Y. M. (2020). "Identifying real energy system solutions to respond to the challenge of climate change," *Energy and Climate Change* 1, article ID 100018. DOI: 10.1016/j.egycc.2020.100018

Christensen, E., Williams, A., Paul, S., Burton, S., and McCormick, R. L. (2011). "Properties and performance of levulinate esters as diesel blend components," *Energy & Fuels* 25(11), 5422-5428. DOI: 10.1021/ef201229j

Di Bucchianico, D. D. M., Wang, Y., Buvat, J. C., Pan, Y., Moreno, V. C. and Leveneur, S. (2022). "Production of levulinic acid and alkyl levulinates: A process insight," *Green Chemistry* 24(2), 614-646. DOI: 10.1039/d1gc02457d

Du, X. Y., Lu, X. B., Bai, H., Xiong, J., Yu, Z. H., Sun, L., and Zhang, R. (2022). "Mesoporous molecular sieves solid superacid as a catalyst for alcoholysis of fructose into methyl levulinate," *Biomass and Bioenergy* 166, article ID 106627. DOI: 10.1016/J.BIOMBIOE.2022.106627

Gupta, S. S. R., and Kantam, M. L. (2019). "Catalytic conversion of furfuryl alcohol or levulinic acid into alkyl levulinates using a sulfonic acid-functionalized hafnium-based MOF," *Catalysis Commun.* 124, 62-66. DOI: 10.1016/j.catcom.2019.03.003

Hronec, M., Fulajtárová, K., and Soták, T. (2014). "Kinetics of high temperature conversion of furfuryl alcohol in water," *Journal of Industrial and Engineering Chemistry* 20(2), 650-655. DOI: 10.1016/j.jiec.2013.05.029

Jia, B. Y., Liu, C., and Qi, X. H. (2020a). "Selective production of ethyl levulinate from levulinic acid by lipase-immobilized mesoporous silica nanoflowers composite," *Fuel Processing Technology* 210, article ID 106578. DOI: 10.1016/j.fuproc.2020.106578

Jia, S., Ma, J., Wang, D., Wang, K., Zheng, Q., Song, C., and Guo, X. (2020b). "Fast and efficient upgrading of levulinic acid into long-chain alkyl levulinate fuel additives with a tungsten salt catalyst at low temperature," *Sustainable Energy & Fuels* 4(4), 2018-2025. DOI: 10.1039/C9SE01287G

Jia, S. Y., Wang, M. C., Ma, J., Liu, X. M., Zhang, Y. J., and Xu, Z. W. (2022). "Metal chloride mediated efficient conversion of hydroxymethylfurfural (HMF) into long-chain levulinate ester," *BioResources* 17(1), 849-861. DOI: 10.15376/biores.17.1.849-861

Kim, T., Assary, R. S., Kim, H., Marshall, C. L., Gosztola, D. J., Curtiss, L. A., and Stair, P. C. (2013). "Effects of solvent on the furfuryl alcohol polymerization reaction: UV Raman spectroscopy study," *Catalysis Today* 205, 60-66. DOI: 10.1016/j.cattod.2012.09.033

Kim, J., and Han, J. (2021). "Bio-based process for the catalytic production of ethyl levulinate from cellulose," *Applied Energy* 300, article ID 117430. DOI: 10.1016/J.APENERGY.2021.117430

Liao, Q., Liang, Y. T., Tu, R. F., Huang, L. Q., Zheng, J. Q., Wang, G. T., and Zhang, H. R. (2022). "Innovations of carbon-neutral petroleum pipeline: A review," *Energy Reports* 8, 13114-13128. DOI: 10.1016/J.EGYR.2022.09.187

Liang, X., Fu, Y., and Chang, J. (2020). "Sustainable production of methyl levulinate from biomass in ionic liquid-methanol system with biomass-based catalyst," *Fuel* 259, article ID 116246. DOI: 10.1016/j.fuel.2019.116246

Li, H., Fang, Z., Smith Jr., R. L., and Yang, S. (2016). "Efficient valorization of biomass to biofuels with bifunctional solid catalytic materials," *Progress in Energy and Combustion Science* 55, 98-194. DOI: 10.1016/j.pecs.2016.04.004

Lomba, L., Muñiz, S., Pino, M. R., Navarro, E., and Giner, B. (2014). "Ecotoxicity studies of the levulinate ester series," *Ecotoxicology* 23, 1484-1493. DOI: 10.1007/s10646-014-1290-y

Pasha, N., Lingaiah, N., and Shiva, R. (2019). "Zirconium exchanged phosphotungstic acid catalysts for esterification of levulinic acid to ethyl levulinate," *Catalysis Letters* 149(9), 2500-2507. DOI: 10.1007/s10562-019-02862-z

Peng, L., Li, H., Long, X., Chen, K., and Chen, H. (2014). "Facile and efficient conversion of furfuryl alcohol into n-butyl levulinate catalyzed by extremely low acid concentration," *BioResources* 9(3), 3825-3834. DOI: 10.15376/biores.9.3.3825-3834

Peng, L. C., Gao, X. Y., and Chen, K. L. (2015). "Catalytic upgrading of renewable furfuryl alcohol to alkyl levulinates using $AlCl_3$ as a facile, efficient, and reusable catalyst," *Fuel* 160, 123-131. DOI: 10.1016/j.fuel.2015.07.086

Sádaba, I., Lima, S., Valente, A., and Manuel, L. G. (2011). "Catalytic dehydration of xylose to furfural: Vanadyl pyrophosphate as source of active soluble species," *Carbohydrate Research* 346(17), 2785-2791. DOI: 10.1016/j.carres.2011.10.001

Sankar, E. S., Reddy, K. S., Jyothi, Y., Raju, B. D., and Rao, K. S. R. (2017). "Alcoholysis of furfuryl alcohol into n-butyl levulinate over SBA-16 supported heteropoly acid catalyst," *Catalysis Letters* 147, 2807-2816. DOI: 10.1007/s10562-017-2155-9

Saravanakumar, A., Vijayakumar, P., Hoang, A. T., Kwon, E. E., and Chen, W.-H. (2023). "Thermochemical conversion of large-size woody biomass for carbon neutrality: Principles, applications, and issues," *Bioresource Technology* 370, Article ID 128562. DOI: 10.1016/j.biortech.2022.128562

Tiwari, M. S., Dicks, J. S., Keogh, J., Ranade, V. V., and Manyar, H. G. (2020). "Direct conversion of furfuryl alcohol to butyl levulinate using tin exchanged tungstophosphoric acid catalysts," *Molecular Catalysis* 488, Article ID 110918. DOI: 10.1016/j.mcat.2020.110918

Xu, S., Pan, D., Wu, Y., Song, X., Gao, L., Li, W., Das, L., and Xiao, G. (2018). "Efficient production of furfural from xylose and wheat straw by bifunctional chromium phosphate catalyst in biphasic systems," *Fuel Processing Technology* 175, 90-96. DOI: 10.1016/j.fuproc.2018.04.005

Wang, G. F., Zhang, Z. Q., and Song, L. H. (2014). "Efficient and selective alcoholysis of furfuryl alcohol to alkyl levulinates catalyzed by double SO_3H-functionalized ionic liquids," *Green Chemistry* 16(3), 1436-1443. DOI: 10.1039/c3gc41693c

Yang, Y., and Kou, Y. (2004). "Determination of the Lewis acidity of ionic liquids by means of an IR spectroscopic probe," *Chemical Communications* 2004(2), 226-227. DOI: 10.1039/B311615H

Yang, X. M., Yang, J. R., Gao, B., Lu, T. L., and Zhou, L. P. (2019). "Conversion of glucose to methyl levulinate over Sn-Al-β zeolite: Role of Sn and mesoporosity," *Catalysis Communications* 130, article ID 105783. DOI: 10.1016/j.catcom.2019.105783

Zhang, Z. H., Dong, K., and Zhao, Z. B. (2011). "Efficient conversion of furfuryl alcohol into alkyl levulinates catalyzed by an organic–inorganic hybrid solid acid catalyst," *ChemSusChem* 4(1), 112-118. DOI: 10.1002/cssc.201000231

Zhang, L. X., Yu, H. B., Wang, P., and Li, Y. (2014). "Production of furfural from xylose, xylan and corncob in gamma-valerolactone using $FeCl_3$• $6H_2O$ as catalyst," *Bioresource Technology* 151, 355-360. DOI: 10.1016/j.biortech.2013.10.099

Zhang, L., Tian, Y. B., Wang, Y., and Dai, L. (2021). "Enhanced conversion of α-cellulose to 5-HMF in aqueous biphasic system catalyzed by $FeCl_3$-$CuCl_2$," *Chinese Chemical Letters* 32(7), 2233-2238. DOI: 10.1016/j.cclet.2020.12.030

Zhang, X., and Li, J. R. (2022). "Recovery of greenhouse gas as cleaner fossil fuel contributes to carbon neutrality," *Green Energy & Environment* 8(2), 351-353. DOI: 10.1016/j.gee.2022.06.002

Zhou, S. L., Lai, J. H., Liu, X., Huang, Z., You, G. L., Xu, Q., and Yin, D. L. (2022). "Selective conversion of biomass-derived furfuryl alcohol into n-butyl levulinate over sulfonic acid functionalized TiO_2 nanotubes," *Green Energy & Environment* 7(2), 257-265. DOI: 10.1016/j.gee.2020.09.009

Zhou, X., Li, Z. X., Zhang, C., Gao, X. P., Dai, Y. Z., and Wang, G. Y. (2016). "Efficient conversion of renewable levulinic acid to n-butyl levulinate catalyzed by ammonium and silver co-doped phosphotungstic acid," *Journal of Molecular Catalysis A: Chemical* 417, 71-75. DOI: 10.1016/j.molcata.2016.03.006

Article submitted: March 15, 2023; Peer review completed: June 10, 2023; Revised version received and accepted: July 6, 2023; Published: July 11, 2023.
DOI: 10.15376/biores.18.3.5765-5776

APPENDIX

Supplementary Material

The Calculation method for GC analysis

A series of standard curves were established for the calculation of FA and levulinate esters with *p*-xylene as the internal standard. The standard curves were listed as follows:

FA: $y=0.492x+0.1541$（$R^2=0.990$）

HL: $y=0.4415x-0.0056$（$R^2=0.997$）

2-Ethylbutyl levulinate: $y=1.049x-0.0058$（$R^2=0.999$）

Hexan-2-yl levulinate: $y=1.0574x-0.0059$（$R^2=0.999$）

Hexan-3-yl levulinate: $y=1.1031x-0.0061$（$R^2=0.999$）

Cyclohexyl levulinate: $y=0.9892x+0.0054$（$R^2=0.999$）

1-Octyl levulinate: $y=1.4051x-0.0078$（$R^2=0.999$）

The y and x values represent to be the peak area ratio of compound to *p*-xylene in GC and the molar ratio of compound to *p*-xylene, respectively.

The calculations for detected FA and HL were taken as the example as below.

N_{FA} (mol)= [（$y-0.1541$）/ 0.492] ×（$m_{p\text{-xylene}}/106.165$）

N_{HL} (mol)= [（$y+0.0056$）/0.4415] ×（$m_{p\text{-xylene}}/106.165$）

Herein, $m_{p\text{-xylene}}$ represents to be the mass of added *p*-xylene, and 106.165 is the molecular weight of *p*-xylene.

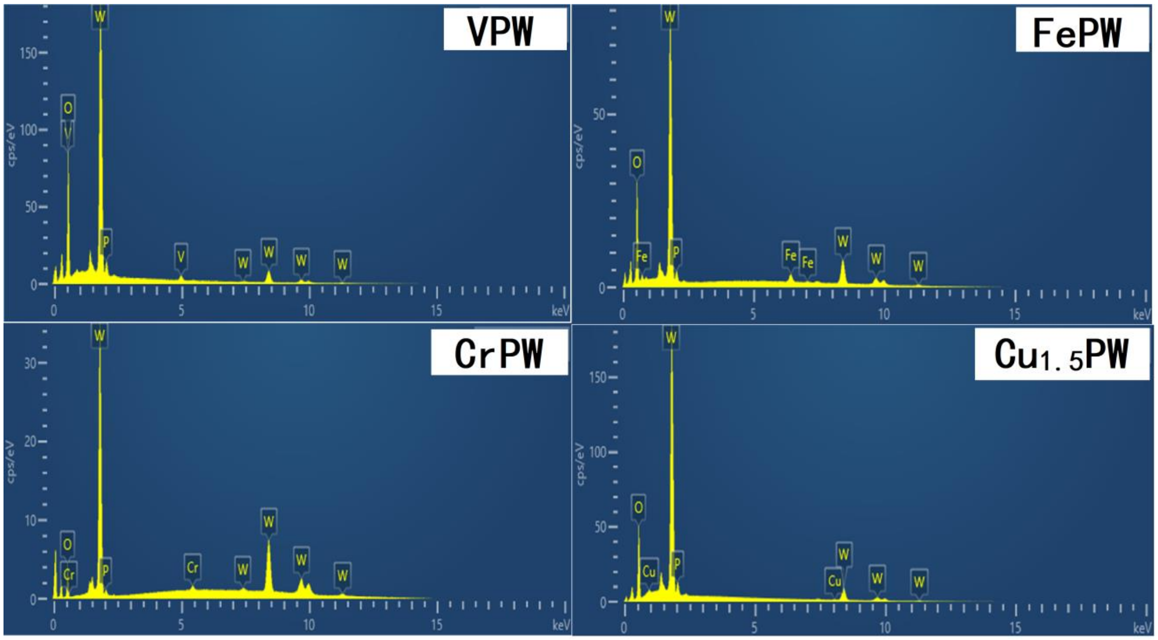

Fig. S1. EDS results for the as-synthesized catalysts